Analysis of Overvoltages Across Line Insulator Strings Considering the Ground-Wire and Phase Conductors Corona

T. M. Pereira, R. Alipio, M. C. Tavares

***Abstract*--This paper assesses the influence of corona effect on the overvoltages developed across the insulator strings of overhead transmission lines due to lightning. The influence of corona is investigated considering lightning strikes to the tower top and shielding wires at midspan. A large range of soil resistivity and lightning currents peaks are evaluated in the analysis, and the stress across the insulator strings is evaluated applying the integration method. Simulations are carried out in the Alternative Transient Program (ATP/EMTP), wherein the corona effect is represented through the accurate Suliciu corona model, which was implemented using the MODELS interface and combined with J. Marti line model. Furthermore, it was also represented the wideband behavior of tower grounding system. Results showed that corona effect has a minor influence in the overvoltages across the insulator string for strikes to the tower top. However, it strongly influences the overvoltages across line insulators ensuing from a lightning strike to the shielding wire at the midspan, leading to a decrease in the peak value of the lightning current that causes line flashover.**

***Keywords*: Corona, lightning overvoltages, insulator strings, transmission lines.**

I. Introduction

FOR most overhead power transmission lines (TLs), lightning is the primary cause of unscheduled interruptions [1]. An accurate assessment of the lightning performance of transmission lines requires the knowledge of both the magnitude and waveform of overvoltages across line insulators. Two main phenomena affect the attenuation and distortion of surge overvoltages propagation along overhead transmission lines: 1) Frequency-dependent losses associated with the ground return impedance and skin effect of aerial conductors, 2) Variation of the shunt parameters due to corona effect [2].

Normally, the economic impact of power supply interruptions is huge, which justifies the several recent studies focused on the lightning performance of transmission lines. However, although these studies consider accurate modeling of power components for lightning studies, most of them disregard the impact of the corona effect on overvoltages [3]–[5]. In other cases, corona is represented in a very simplified way. For instance, in IEEE FLASH [1], possibly the most used platform for estimating the line performance in industry, corona is represented by a simple constant increase in conductor radius and a modification of line capacitance. This methodology is very limited, mainly for lightning overvoltage studies, since it disregards all the dynamic and complexity relating of the phenomenon, which include nonlinear, hysteretic and frequency-dependent characteristics [6].

As well-established in the literature, the insulation flashover does not depend only on the magnitude of overvoltages, but it is also strongly influenced by the voltage waveform. Thus, to assess the line insulation breakdown due to lightning overvoltages it is very important that both the magnitude and the waveform of the impinging overvoltages are determined as accurately as possible. Since the corona effect has a relevant role in the attenuation and distortion of travelling waves [2], an accurate representation of this phenomenon is crucial to obtain proper results.

In view of the above presented, this paper assesses the influence of corona effect on the transient voltages across insulators of a transmission line struck by lightning. This is achieved by representing the line components and phenomena with high accurate models in an EMT-type platform, considering the frequency-dependence of line parameters and the wideband behavior of the tower-foot grounding system. The corona effect is represented through the Suliciu corona model [7], which represents the nonlinear, hysteretic and frequency dependence of phenomenon with good accuracy. Sensitivity analyzes are carried out in order to determine the influence of the corona effect on the critical current that leads to line flashover, considering different values of soil resistivity. The main contribution of the work is to demonstrate that in some situations, notably for lightning strike to the midspan, the corona phenomenon leads to an increase of the resulting overvoltages across line insulators. The reasons that lead to this increase in overvoltages are investigated and explained in the paper.

The paper is structured as follows. Section II presents the system under study and modeling guidelines. Section III describes the corona model and its respective implementation in EMT-type platform. Section IV presents the results in terms of the developed lightning overvoltages across line insulators

---

This work was supported in part by the Coordenação de Aperfeiçoamento de Pessoal de Nível Superior - Brasil (CAPES) - Finance Code 001, CNPq (307237-2020/6) and FAPESP (2022/01896-7, 2019/20311-7), Brazil.

Thassio Matias Pereira is with Electrical and Computing Engineering School, University of Campinas, SP, 13083850 Brazil (email: t209420@dac.unicamp.br). Rafael Alipio is with the Department of Electrical Engineering, Federal Center of Technological Education, Belo Horizonte, MG, Brazil (email: Rafael.alipio@cefetmg.br). Maria Cristina Tavares is with Electrical and Computing Engineering School, University of Campinas, SP, 13083850 Brazil (email: ctavares@unicamp.br).

Paper submitted to the International Conference on Power Systems Transients (IPST2023) in Thessaloniki, Greece, June 12-15, 2023.

and critical currents, assuming lightning strikes to both tower top and midspan. Section V discusses the impact of the results in the backflashover rate calculation. Finally, Section VI presents the conclusions.

II. System Under Study

To assess the influence of corona effect on the resulting lightning overvoltages across insulator strings, a typical 230-kV overhead transmission line is considered. Fig. 1 shows the tower design. This line has one conductor ACSR per phase (3.048 cm diameter) and two ACSR shield wires (1 cm diameter). The coordinates of the line cables (in meters) are indicated in the same figures (values within parenthesis are midspan heights). The Critical Flashover Overvoltage (CFO) of the line is 1095 kV. It is worth noting that lines with higher voltage levels have higher CFOs and lightning overvoltages become less of a concern. This justifies the adoption of a 230 kV line for the analyzes presented in this work.

Since the interest of this work relies on the backflashover phenomena, two different strike points are considered in simulations: at the tower top and on the shield wire at the midspan. All simulations presented in this paper have been carried out in the Alternative Transients Program (ATP) [8]. In the next subsections, the modeling of each component of the transmission system is briefly described.

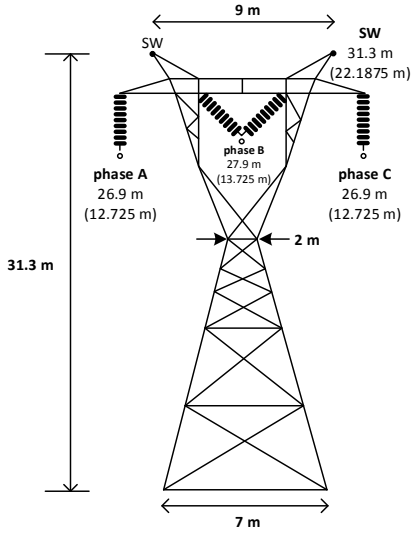

Fig. 1. Typical 230-kV transmission line.

A. Lightning Current Waveform

According to measurements performed in instrumented towers, first return stroke currents of downward negative flashes, which are the most relevant in terms of lightning performance of TLs, are characterized by a concave rising front and maximum steepness near the current peak. Considering these aspects, the lightning current was represented by the concave waveform using a Heidler function with front time of 3.8 μs and time to half-peak of 75 μs. These parameters are consistent with characteristics of first stroke currents of downward negative flashes measured by Berger at Mount San Salvatore (MSS) [9]. The amplitude of the current was varied from 30 kA to 150 kA. In ATP, the lightning current is modelled as a Norton equivalent circuit including an ideal current source in parallel with a lightning-channel impedance Z_{ch} assumed to be constant and equal to 400 Ω, as suggested in [10] for backflashover studies.

B. Transmission Line Model

Transmission line is represented in ATP through the frequency-dependent J.Marti line model. Two 450-m spans were considered at each side of the striking point. Long lines were connected to the external towers to avoid reflections that could affect the simulated overvoltages. Corona effect was modelled as described in Section III.

C. Tower Model

The towers are represented as single-phase distributed-parameter lines, as recommended in CIGRE procedures for estimating the lightning performance of transmission lines [11]. Considering the tower geometry depicted in Fig. 1, the well-known expression for waisted towers was used to compute its surge impedance [11]; a value of $Z_T = 117.5\ \Omega$ was determined according to the tower dimensions. The travel time along the tower was assumed to be $0.85c$, where c is the speed of light, to approximately consider the additional mean path length presented by the crossarms.

D. Tower-foot Grounding Model

The grounding system of the tower is illustrated in Fig. 2. It consists of four counterpoise wires of 0.9525-cm diameter, buried 0.8 m deep in soil. The total length L of the counterpoise wires is selected according to the value of the low-frequency soil resistivity ρ_0, as indicated in Table I. First, the input impedance $Z(j\omega)$ of the tower-footing grounding seen from the bottom of the tower is computed using an accurate electromagnetic model [12]. Calculations were carried out in a frequency range from 10 Hz to 10 MHz, along which the soil resistivity and permittivity are assumed to vary with frequency according to the Alipio-Visacro model [13]. Finally, from the computed input impedance $Z(j\omega)$, a pole-residue model of the associated admittance $Y(j\omega) = 1/Z(j\omega)$ is obtained and incorporated in the ATP time-domain simulations through an equivalent circuit as detailed in [14], [15].

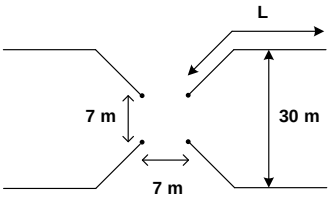

Fig. 2. Typical arrangement of tower-footing grounding electrodes.

TABLE I
LENGTH OF THE COUNTERPOISE WIRES AS A FUNCTION OF SOIL RESISTIVITY

ρ_0 (Ωm)	300	1000	3000	5000
L (m)	15	50	70	90

E. Insulation Flashover

The integration model, also known as disruptive effect (DE) model, is used to determine if an insulation flashover will occur due to the lightning overvoltages. The general equation for computing the disruptive effect associated to a nonstandard overvoltage $e(t)$ across the line insulator is given by (1),

where t_0 is the instant of time when $e(t)$ exceeds the onset voltage V_0, i.e., the minimum voltage to start the breakdown process. If DE given by (1) exceeds the critical disruptive effect (DE_C) associated with a given insulation configuration, a flashover occurs. The peak value of the lightning current that produces an overvoltage with a DE exceeding the DE_C of the line insulator, i.e., leading to line flashover, is called critical current I_{crit}.

$$DE = \int_{t_0}^{t} [e(t) - V_0]^{k_d} dt \qquad (1)$$

As recommended in [2], for a typical 230 kV line with $CFO = 1095$ kV, the following constants are adopted for the DE model: $DE_C = 1.1506(CFO)^{k_d}$, $k_d = 1.36$, and $\frac{V_0}{CFO} = 0.77$.

III. CORONA MODELLING

A. Representation in EMT-type platforms

The available line models in the ATP software, as well as in others EMT-type platforms, disregard the occurrence of the corona effect in transmission lines, and the line is modelled as a linear component. In this way, the representation of the phenomenon can only be done through lumped and external elements to the line. To approximately represent the distributed nature of corona, the line must be discretized into many sections, and at each junction node it is disposed a shunt bus that represents the phenomenon according to the adopted corona model (Fig. 3). In this work, the Suliciu corona model was adopted. From the point of view of accuracy, this model has important advantages in relation of other models. More details are provided in the next section. The transmission line was discretized into section of d=25 m to properly represent the distributed nature of corona effect.

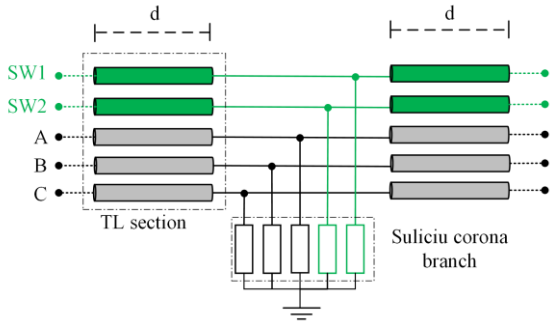

Fig. 3. Representation of corona effect in EMT-type platforms.

B. Suliciu Corona Model

The physical phenomenon of corona is very complex. It includes ionization, effects of mobility, diffusion, deionization and the mutual effect of space charges and electric field [16]. All these phenomena are very difficult to be separately modelled for practical application. For this reason, instead of modeling each microscopic phenomenon separately, the corona models developed for application in EMT-type programs are based on a macroscopic description through the charge-voltage (q-v) diagrams, also known as q-v curves (see Fig. 4). In a simple way, the q-v curve relates the conductor voltage to the resulting space charge and synthesizes the main information needed for the representation of corona effect in transmission lines. The tangent line to the curve is the conductor capacitance, and the area enclosed by the curve is equal to corona losses. Then, an accurate corona model consists of obtaining an accurate representation of the q-v curve. Furthermore, the information synthesized in q-v curve can also be used to determine the variation of capacitive coupling caused by the corona effect in multiphase lines, as shown in shown in [17]–[19].

In EMT-type programs, the nonlinear and hysteretic characteristics of q-v curve can be represented through mathematical equations or approximated by circuit elements (static analogue models) [20]. However, as shown in field measurements data [21], the shape of the q-v curve is wave-front-time dependent, being this characteristic more notable for fast-front overvoltages as caused by lightning. In this context, the Suliciu corona model has a better performance (also known as dynamic corona model) [7]. Basically, the main advantage over others static corona models consists in the fact that, using a rate-type constitutive equation and a set of parameters fitted by measured q-v curves, the Suliciu model can represent with good accuracy the nonlinear, hysteretic and wave-front-time dependence of q-v curves, ensuring the accuracy and reliability of the results obtained in the simulations. This is the most accurate corona model for EMT-type applications, as has been extensively expressed in several works over the years [18], [20], [22] – [30].

For positive and negative polarity voltages, the Suliciu's model equations are presented in (2) - (3). In these equations, i_c is the corona current; Q_c is the corona charge; V is the conductor voltage; C_0 is the geometric capacitance; C_j, V_j and k_j are model parameters, which should be fitted through measured q-v curves, as explained in [7].

$$i_c = \frac{\partial Q_c}{\partial t} = \begin{cases} \left.\begin{matrix} 0, & if\ g_2 \le 0 \\ g_2, & if\ g_1 \le 0 < g_2 \\ g_1 + g_2, & if\ g_1 > 0 \end{matrix}\right\} & V > 0 \\ \left.\begin{matrix} 0, & if\ g_4 \ge 0 \\ g_4, & if\ g_4 < 0 \le g_3 \\ g_3 + g_4, & if\ g_3 < 0 \end{matrix}\right\} & V \le 0 \end{cases} \qquad (2)$$

$$g_j = k_j\left[\left(C_j - C_0\right)\left(V - V_j\right) - Q_c\right], \qquad j = 1, \ldots, 4 \qquad (3)$$

Clearly, the Suliciu model only can be applied if there exist measurements of q-v curves for the line conductors. Unfortunately, these measurements are difficult to be found in literature. However, it was found for phase and shield wire conductors of the 230 kV line adopted in this work [21],[31]. As described in section II, in the TL of Fig. 1 the phase wires are represented by an ACSR 3.048 cm diameter conductor, and the shield wires are represented by an ACSR 1 cm diameter conductor. By means of measured q-v curves, the Suliciu's model parameters were fitted, and comparisons between the measured and calculated q-v curves are shown in Fig. 4. As can

be seen, the results are quite adherent. The values of the parameters are given in Table II.

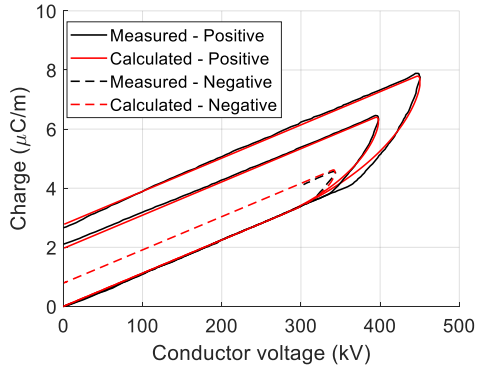

(a) 3.048 cm diameter conductor (phase wire). Measurements presented in [21].

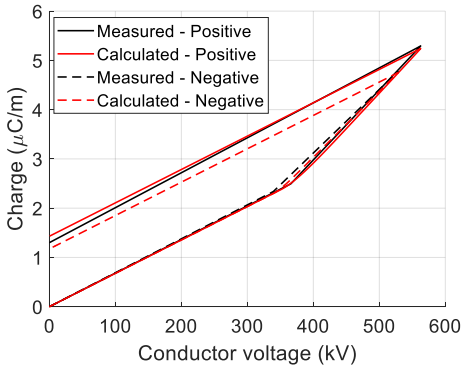

(b) 1 cm conductor diameter (shield wire). Measurements presented in [31].

Fig. 4. Adjustment of the q-v curves using the Suliciu corona model. (a) 3.048 cm diameter conductor (phase wire). (b) 1 cm diameter conductor (shield wire).

TABLE II
SULICIU MODEL PARAMETERS

	Phase wire				Shield wire			
C_0(pF/m)	11.2				6.8			
	1	2	3	4	1	2	3	4
C_j(pF/m)	27	40	27	40	13	15	13	14
V_j(kV)	267	246	-289	-253	350	300	-340	-300
k_j(Hz)	1.4e6	1	1.4e6	1	4e7	0.1	8e7	0.1

It is worth mentioning that the measured curves shown in Fig. 4 were obtained in laboratory tests through corona cages. However, the geometric capacitance of the conductor on overhead transmission line is different from the conductor on the cage. For this reason, if the Suliciu's model parameters C_j, V_j and k_j were tuned for the conductor on the cage, they should be corrected to the conductor on overhead line, which can be done by means of (4) – (7) [23]. In these equations, the superscript l indicates the parameters corrected to overhead line, C_s is the geometric capacitance of the conductor on overhead line and C_0 is the geometric capacitance of the conductor on the cage.

Finally, the Suliciu corona model was implemented in ATP using the Models interface and voltage controlled current sources. Both positive and negative polarity of q-v curves were represented in the simulations. Further details about the implementation of Suliciu corona model for multiphase lines in EMT-type platforms are described in [18].

$$k_j^l = k_j(1 + P_r C_j)\frac{C_s}{C_0} \tag{4}$$

$$C_j^l = C_s + \frac{(C_j - C_0)C_s}{(1 + P_r C_j)C_0} \tag{5}$$

$$V_j^l = V_j \frac{C_0}{C_s} \tag{6}$$

$$P_r = \frac{1}{C_s} - \frac{1}{C_0} \tag{7}$$

IV. RESULTS

A. Lightning Strike at the Tower Top

Fig. 5 shows the overvoltage across the insulator string of phase C, considering and neglecting the corona effect, yielded by a direct strike of a 100-kA lightning current at the tower top. For simplicity, waveforms are shown only for the insulator string related to the phase C, since it presents the highest overvoltages (worst-case).

When a lightning strikes the tower top, the current is divided into three parcels, two that go through the shielding wires and one that goes down the tower. The later parcel produces a voltage wave along the tower that is transmitted to its crossarms. Also, voltages are induced at the phase conductors. The surge voltage resultant at each line insulator string is the difference between the crossarm voltage and the voltage coupled to the phase conductor from the tower top and shielding wires. During the first microseconds of the transient, the crossarm voltages, and therefore the voltages across line insulators, are mostly determined by the reflections that take place at the tower top and at the tower-foot grounding system. At later times, the insulator voltages are also influenced by reflections coming from the adjacent towers.

According to the results, the peak value of the overvoltages is only slightly affected when the corona effect is included, being observed a decrease of around 5%, which is roughly independent of the soil resistivity. This stems from the fact that, for a direct strike at the top of the tower, the peak value of the resultant overvoltages is basically determined by the reflected wave at the bottom of the tower, which is ultimately related with the tower-foot grounding system.

Considering typical spans lengths, reflections coming from the adjacent towers are likely to influence the overvoltages across line insulators only after the peak value. These reflected waves are subject to attenuation and distortion when traveling along the span due to both frequency-dependent line parameters and corona effects. This explains the more noticeable differences observed along the wave tail of the curves calculated considering or neglecting the corona effect. The reduction in the overvoltage peak value is presumably due to the increased share of current diverted to the shield wire when in corona due to the reduction of its surge impedance. However, due to the dynamic nature of the implemented corona model, the corona effect on the shield wire has little influence in the first few microseconds and becomes increasingly more important as the overvoltage grows and approaches its peak

value. For this reason, although the shield wire conducts a greater share of the lightning current when in corona, this effect has only a moderate impact on reducing the peak value of the resulting overvoltage. This is because the effect becomes relevant at times when the overvoltage is already close to its peak value.

It is to be noted that the insulator flashover occurrence depends not only on the peak value of the overvoltage, but also on its waveform. Thus, to give generality to the findings, results similar to those shown in Fig. 5 were obtained by varying the current amplitude between 30 kA and 150 kA and the disruptive effect associated with each resulting overvoltage in phase C was calculated. The results obtained are shown in Fig. 6 for the four different values of soil resistivity between 300 Ωm and 5000 Ωm, covering from low- to very high-resistivity soils.

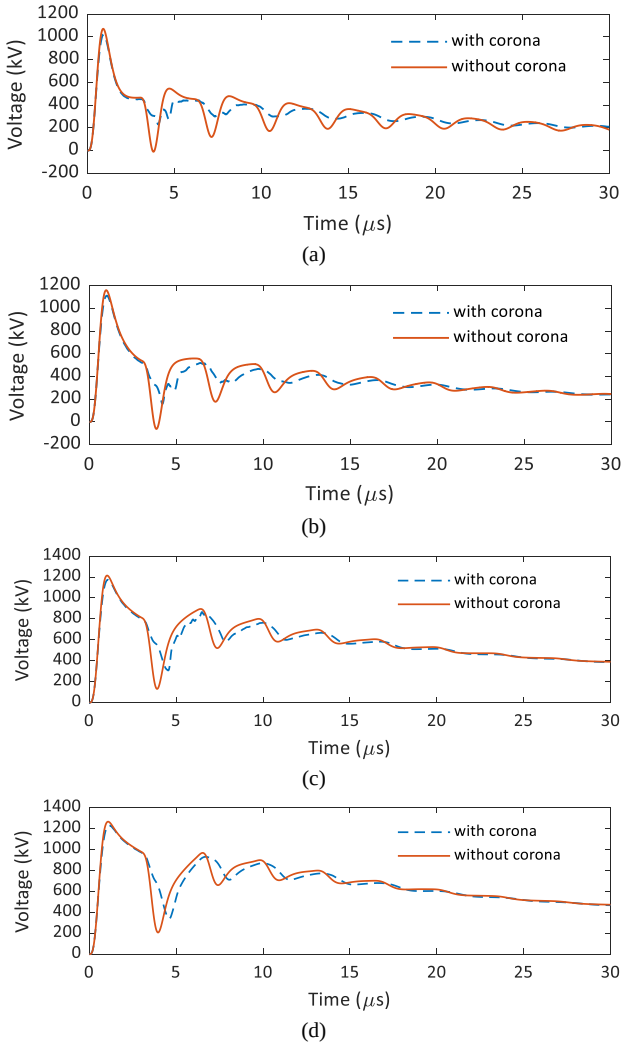

Fig. 5. Voltages across the insulator string of phase C for current injection of 100-kA to the tower top, considering or neglecting the corona effect, for a soil resistivity of (a) 300 **Ω**m, (b) 1000 **Ω**m, (c) 3000 **Ω**m, and (d) 5000 **Ω**m.

The disruptive effects computed considering the corona effect is only slightly inferior to that obtained disregarding the phenomenon. This result is maintained for a wide range of currents and considering different values of soil resistivity and tower-foot grounding conditions. Consequently, the critical current, that is, the current that yields line flashover, is only slightly higher when the corona effect is included. It is worth noting that for resistivities of 300 Ωm and 1000 Ωm, the critical current is greater than 150 kA.

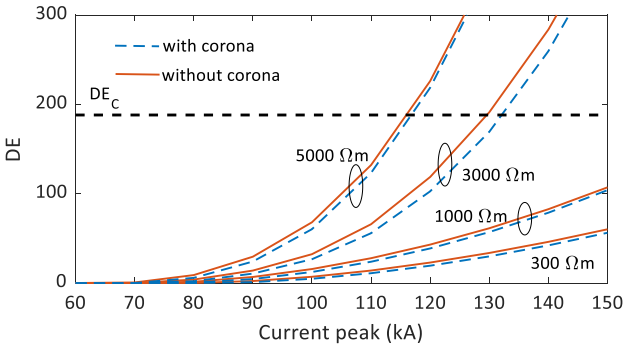

Fig. 6. Disruptive effect as a function of the lightning current peak for current injection at the tower top.

B. Lightning Stroke at the Midspan

In this section, a direct strike to the shielding wire at midspan is assumed and the ensuing overvoltages across the insulator strings at the tower are computed. The main objective is to assess the influence of corona effect on the probability of flashover at the tower due to lightning strokes hitting the line at the midspan. It should be emphasized that the phenomena of flashover within the span was not analyzed in this paper. In fact, according to [32], although flashover within the span is possible, such a phenomenon is insignificant compared to flashovers at the tower due, among other factors, to the flow of pre-discharge currents from the shield wire to the phase conductor producing a voltage on the phase conductor which reduces the voltage across the span insulation.

Fig. 7 shows the resultant overvoltages across the insulator string of the phase C, considering and neglecting the corona effect, and assuming a 100-kA peak current. According to the results, larger deviations are observed between the voltage waveforms calculated considering and neglecting corona, in comparison with the previous case of lightning strike to the tower top. It is seen that considering the corona effect, the waveforms are more damped and distorted along their late-time response. Interestingly, along the overvoltage wavefront, higher peak values are observed if the corona effect is considered in simulations.

To better understand these interesting results, Fig. 8 compares the voltages at the tower top and at phase C, both in relation to remote earth, calculated considering and neglecting the corona effect for a 3000-Ωm soil. When the lightning strikes the shielding wire at the midspan, the associated voltage waves propagate towards the adjacent towers, as well as the voltage waves induced in the phase conductors. When these waves reach the tower, overvoltages are developed across line insulators, which correspond approximately to the difference between the voltage wave at the top of the tower and the induced voltages at the phase conductors. Thus, the larger differences between the calculated overvoltages across insulators considering or neglecting corona can be readily explained as a result of different distortion and attenuation experienced by the propagating waves through the shield wires and phase conductors due to corona. In particular, the larger

negative peak of the induced voltage at the phase conductor during the first microseconds observed when the corona effect is considered explains the higher peaks of overvoltages across insulator strings, compared to the curves where corona is disregarded.

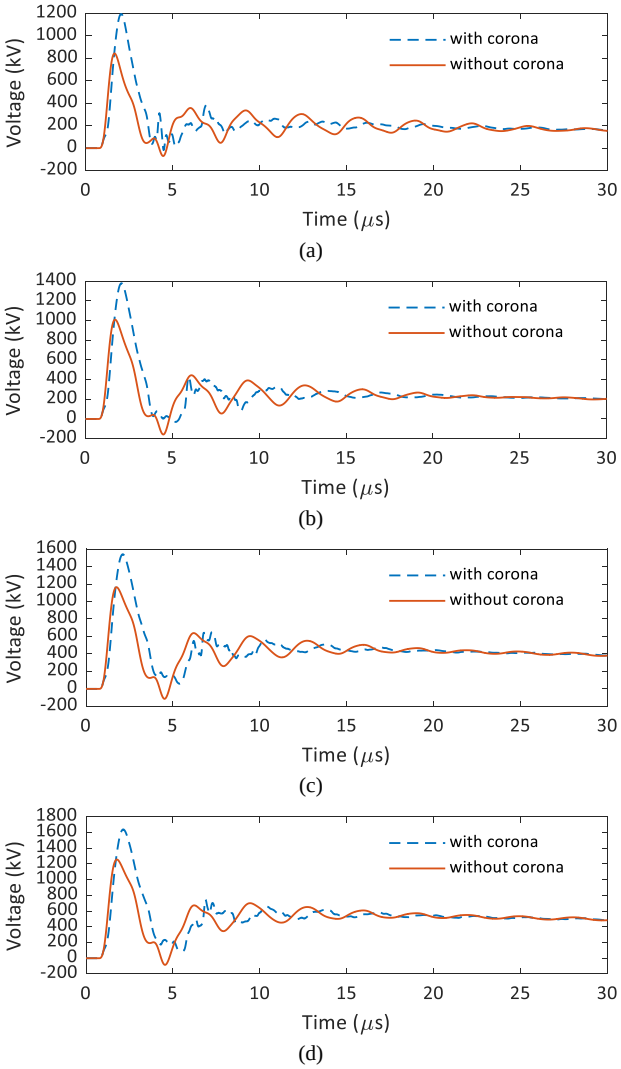

Fig. 7. Voltages across the insulator string of phase C of the first tower on the left of the strike point, for a current injection of 100-kA at the shield wire at midspan, considering or neglecting the corona effect, for a soil resistivity of (a) 300 **Ω**m, (b) 1000 **Ω**m, (c) 3000 **Ω**m, and (d) 5000 **Ω**m.

To evaluate the impact of the results obtained on the critical current that yields line flashover, results like those shown in Fig. 6 were obtained for 30-kA to 150-kA current amplitudes and the disruptive effect associated with each resulting overvoltage in phase C was calculated. The results obtained are shown in Fig. 9 for resistivities between 300 Ωm and 5000 Ωm.

Comparing the results of Fig. 6 with those of Fig. 9, it is seen that the lightning strike to the tower top leads to much more severe overvoltages (higher DE) across line insulators in comparison with strike to midspan when the corona effect is disregarded. In fact, comparing the curves of Fig. 6 and Fig. 9 for the same values of soil resistivity and neglecting corona effect, the strike to the midspan leads to DE values approximately half of those resulting from the incidence at the tower top. For instance, for the 5000-Ωm soil, even the direct strike of a 150-kA current at the midspan does not cause line flashover.

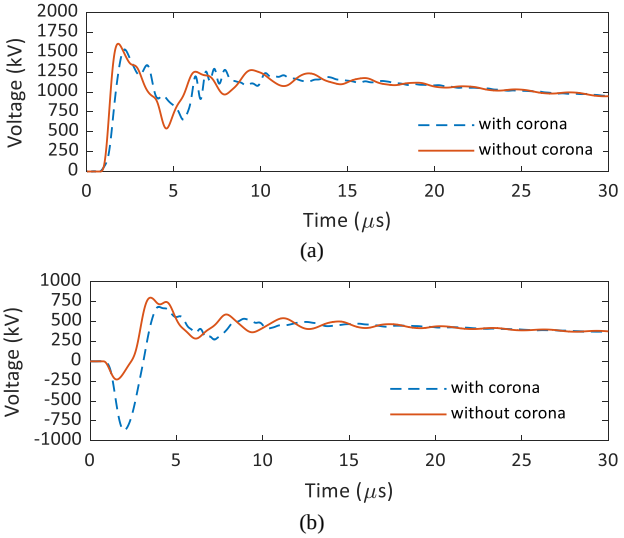

Fig. 8. Voltages (a) at the top of the tower, (b) at the phase C, for a current injection to the shield wire at midspan, considering or neglecting the corona effect, for 3000-**Ω**m soil.

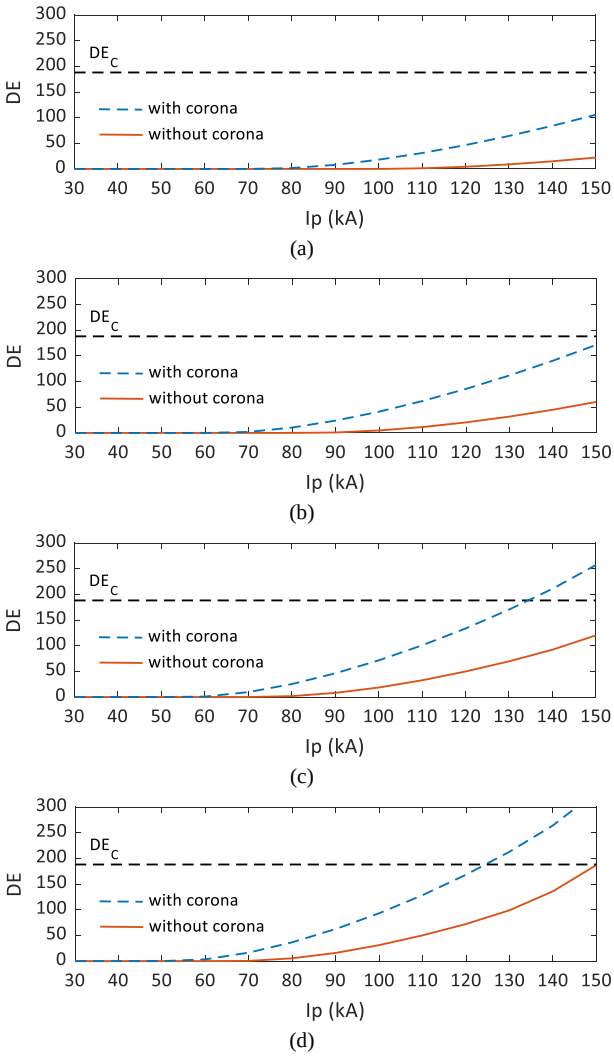

Fig. 9. Disruptive effect as a function of the lightning current peak for current injection at the shield wire at midspan, for a soil resistivity of (a) 300 **Ω**m, (b) 1000 **Ω**m, (c) 3000 **Ω**m, and (d) 5000 **Ω**m.

On the other hand, when the corona effect is included in simulations, much higher DE values are obtained, in accordance with the results of overvoltages across line insulators which show higher peaks in comparison with the results neglecting corona. As a result, much lower critical current values are obtained, which are comparable to those calculated for lightning strike to the tower top. More importantly, the results obtained show that when the corona effect is considered, a greater probability of line flashover due to strikes to the midspan is predicted.

V. DISCUSSION

Traditionally, the annual backflashover rate per 100 km of a transmission line, BFR, is estimated by the following expression:

$$BFR = 0.6 \cdot N_{LT} \cdot P(I > I_{crit}) \quad (8)$$

where $P(I > I_{crit})$ is the probability of the lightning peak current being greater than the minimum current that causes insulation flashover and N_{LT} is the annual number of flashes to the line per 100 km. In this traditional calculation, only lightning strikes to the tower top are considered and the so-called span factor of 0.6 is adopted for disregarding the effect of strokes along the span. That is, it is assumed that 60% of the flashes contacting the line will hit the tower, and that the remaining 40% terminating within the span would lead to overvoltages across the insulator strings with a low probability of causing insulation flashover. It is noteworthy that expression (8) does not consider the occurrence of flashovers within the span to compose the total line backflashover rate since, as mentioned earlier, this phenomenon is insignificant compared to flashovers at the tower.

Indeed, considering the results of section IV-B, when the corona effect is neglected, very high values of critical current are found for lightning strikes to the midspan, indicating a low probability of insulation flashover. In such cases, the use of the span factor seems to be justified. However, when the corona effect is considered, much lower values of critical current are found, of the same order of magnitude as those obtained for lightning incidence at the tower top for the same grounding conditions. In this case, the use of the span factor would lead to an underestimation of line annual outage rate.

In the light of the above discussion, the use of the span factor should be viewed with caution. A better procedure would be to calculate the BFR for both a stroke to the tower and for strokes along the span, and finally sum them to obtain the total line outage rate. In calculating the BFR for strokes within the span, the corona effect should not be neglected.

VI. CONCLUSIONS

In this paper, the influence of corona effect in lightning overvoltages across the insulator strings of a 230 kV transmission line was investigated. The system was modeled in an EMT-type platform, where the behavior of transmission line, corona effect and tower-foot ground system were represented through accurate models.

For lightning strikes to the tower top, it was shown that corona has low influence in the impinging overvoltages across line insulators, being observed a decrease of around 5 % in their peak values independently of the soil resistivity. This stems from the fact that, for a direct strike at the top of the tower, the peak value of the resultant overvoltages is basically determined by the reflected wave at the bottom of the tower, which is ultimately related with the tower grounding system. For lightning strikes to the shielding wire at mid-span, however, it was shown that corona effect has a great influence in the resultant lightning overvoltages, leading to a decrease of the critical current that causes line flashover. This result stems from a larger voltage of opposite polarity induced in the phase conductors, when corona effect is considered. The obtained results show that, when calculating the lightning overvoltages due to strokes within the span, the corona effect should not be neglected, and more accurate formulations should be developed for the annual backflashover rate estimation.

In forthcoming material, the influence of the corona effect on the overvoltages across insulator strings will be analyzed for others tower geometries, including vertical double circuits structures. Furthermore, new formulations for estimation of the annual BFR will be proposed.

VII. REFERENCES

[1] IEEE Std 1243-1997, *IEEE guide for Improving the lightning performance of Transmission Lines*. 1997. doi: 10.1109/IEEESTD.1997.84660.

[2] A. R. Hileman, *Insulation Coordination for Power Systems*, 1st ed. Washington, D. C.: CRC Press, 1999.

[3] R. Shariatinasab, J. Gholinezhad, and K. Sheshyekani, "Estimation of Energy Stress of Surge Arresters Considering the High-Frequency Behavior of Grounding Systems," *IEEE Trans Electromagn Compat*, vol. 60, no. 4, pp. 917–925, 2018, doi: 10.1109/TEMC.2017.2756700.

[4] F. H. Silveira and S. Visacro, "Lightning Performance of Transmission Lines: Impact of Current Waveform and Front-Time on Backflashover Occurrence," *IEEE Transactions on Power Delivery*, vol. 34, no. 6, pp. 2145–2151, 2019, doi: 10.1109/TPWRD.2019.2897892.

[5] Z. Datsios, P. Mikropoulos, and T. Tsovilis, "Closed-Form Expressions for the Estimation of the Minimum Backflashover Current of Overhead Transmission Lines," *IEEE Transactions on Power Delivery*, vol. 36, no. 2, pp. 1–1, 2020, doi: 10.1109/tpwrd.2020.2984423.

[6] J. A. Martinez-Velasco, *Power System Transients: Parameter Determination*. CRC Press, 2010.

[7] M. Mihăilescu-Suliciu and I. Suliciu, "A rate type constitutive equation for the description of the corona effect," *IEEE Transactions on Power Apparatus and Systems*, vol. PAS-100, no. 8, pp. 3681–3685, 1981, doi: 10.1109/TPAS.1981.317010.

[8] EMTP User Group, *Alternative Transients Program (ATP): Rule Book, Can./Amer. EMTP User Group, Leuven EMTP Center, Leuven, Belgium*. 1987.

[9] K. Berger, R. B. Anderson, and H. Kroninger, "Parameters of lightning flashes," *Electra*, no. 80, pp. 223–237, 1975.

[10] Z. G. Datsios, P. N. Mikropoulos, and T. E. Tsovilis, "Effects of Lightning Channel Equivalent Impedance on Lightning Performance of Overhead Transmission Lines," *IEEE Trans Electromagn Compat*, vol. 61, no. 3, pp. 623–630, Jun. 2019, doi: 10.1109/TEMC.2019.2900420.

[11] "Working Group C4.23 - CIGRE TB 839: Procedures for Estimating the Lightning Performance of Transmission Lines – New Aspects," Paris, 2021.

[12] S. Visacro and A. Soares, "HEM: A model for simulation of lightning-related engineering problems," *IEEE Transactions on Power Delivery*, vol. 20, no. 2 I, pp. 1206–1208, 2005, doi: 10.1109/TPWRD.2004.839743.

[13] R. Alipio and S. Visacro, "Modeling the frequency dependence of electrical parameters of soil," *IEEE Trans Electromagn Compat*, vol. 56, no. 5, pp. 1163–1171, 2014, doi: 10.1109/TEMC.2014.2313977.

[14] B. Gustavsen and A. Semlyen, “Rational approximation of frequency domain responses by vector fitting,” *IEEE Transactions on Power Delivery*, vol. 14, no. 3, pp. 1052–1061, Jul. 1999, doi: 10.1109/61.772353.
[15] B. Gustavsen, “Computer code for rational approximation of frequency dependent admittance matrices,” *IEEE Transactions on Power Delivery*, vol. 17, no. 4, pp. 1093–1098, Oct. 2002, doi: 10.1109/TPWRD.2002.803829.
[16] C. Jesus and M. T. C. Barros, “Modelling of corona dynamics for surge propagation studies,” *IEEE Transactions on Power Delivery*, vol. 9, no. 3, pp. 1564–1569, 1994, doi: 10.1109/61.311209.
[17] M. T. C. de Barros, “Identification of the capacitance coefficients of multiphase transmission lines exhibiting corona under transient conditions,” *IEEE Transactions on Power Delivery*, vol. 10, no. 3, pp. 1642–1648, 1995, doi: 10.1109/61.400951.
[18] H. M. Barros, S. Carneiro, and R. M. Azevedo, “An efficient recursive scheme for the simulation of overvoltages on multiphase systems under corona,” *IEEE Transactions on Power Delivery*, vol. 10, no. 3, pp. 1443–1452, Jul. 1995, doi: 10.1109/61.400928.
[19] T. Noda, “Development of a Transmission-line Model Considering the Skin and Corona Effects for Power Systems Transient Analysis,” Doshisha University, Kyoto, Japan, 1996.
[20] S. Carneiro and J. R. Marti, “Evaluation of corona and line models in electromagnetic transients simulations,” *IEEE Transactions on Power Delivery*, vol. 6, no. 1, pp. 334–342, 1991, doi: 10.1109/61.103756.
[21] P. S. Maruvada, H. Menemenlis, and R. Malewski, “Corona characteristics of conductor bundles under impulse voltages,” *IEEE Transactions on Power Apparatus and Systems*, vol. 96, no. 1, pp. 102–115, Jan. 1977, doi: 10.1109/T-PAS.1977.32313.
[22] S. Carneiro, J. R. Marti, H. W. Dommel, and H. M. Barros, “An efficient procedure for the implementation of corona models in electromagnetic transients programs,” *IEEE Transactions on Power Delivery*, vol. 9, no. 2, pp. 849–855, Apr. 1994, doi: 10.1109/61.296266.
[23] H. Hamadani-Zadeh, “Dynamic Corona model and frequency dependent line model for EMTP (IREQ report - Institut de recherche d’Hydro-Québec),” 1986.
[24] P. S. Maruvada, D. H. Nguyen, and H. Hamadani-Zadeh, “Studies on modeling corona attenuation of dynamic overvoltages,” *IEEE Transactions on Power Delivery*, vol. 4, no. 2, pp. 1441–1449, 1989, doi: 10.1109/61.25631.
[25] J. Mahseredjian, “Corona model - EMTP-RV User’s Guide,” Montreal, Canada, 2016.
[26] P. Lacasse and J. Mahseredjian, “Implementation of a Multiphase Corona Line Model in the EMTP User’s Manual, IREQ Report 94-326,” 1994.
[27] J. Mahseredjian, “Support Routine for the EMTP Dynamic Corona Model, IREQ Report - 4534,” 1989.
[28] M. Cervantes *et al.*, “Simulation of Switching Overvoltages and Validation With Field Tests,” *IEEE Transactions on Power Delivery*, vol. 33, no. 6, pp. 2884–2893, Dec. 2018, doi: 10.1109/TPWRD.2018.2834138.
[29] K. Huang, X. Zhang, and S. Tao, “Electromagnetic Transient Analysis of Overhead lines Including Corona and Frequency Dependence Effects under Damped oscillation Surges,” *IEEE Transactions on Power Delivery*, vol. 33, no. 5, pp. 2198–2206, 2018, doi: 10.1109/TPWRD.2018.2794825.
[30] T. M. Pereira, J. S. Acosta, J. A. Santiago, and M. C. Tavares, “Overvoltages due to line faults on HWL transmission Line: Corona effect and mitigation techniques,” in *Submitted to International Conference of Power System Transients (IPST 2023)*, 2023.
[31] C. Gary, G. Dragan, and D. Cristescu, “Attenuation of travelling waves caused by corona,” in *International Conference on Large High Voltage Eletric Systems*, 1978.
[32] CIGRE, “Guide to procedures for estimating the lightning performance of transmission lines - Working Group 01 (Lightning) of Study Committee 33 (Overvoltages and Insulation Coordination),” 1991, vol. 01, no. October, p. 63.